Supplementary Appendix

This appendix has been provided by the authors to give readers additional information about their work.

Supplement to: Antonarakis ES, Lu C, Wang H, et al. AR-V7 and resistance to enzalutamide and abiraterone in prostate cancer. N Engl J Med 2014;371:1028-38. DOI: 10.1056/NEJMoa1315815

Supplementary Appendix

Table of Contents

Methods

Analysis of circulating tumor cells

CTC analyses were conducted using the commercially-available AlereTM CTC AdnaTest platform (AdnaGen, Langenhagen, Germany). This assay does not enable CTC enumeration. Isolation and enrichment of CTCs was performed using the ProstateCancerSelect kit, and mRNA expression analyses were performed using the ProstateCancerDetect kit with multiplexed reverse-transcription polymerase-chain-reaction (qRT-PCR) primers to detect the presence of CTCs, and custom primers designed to detect the full-length-AR (AR-FL) and AR splice variant-7 (AR-V7). [1,2] The relative AR-V7 transcript abundance was determined by calculating the ratio of AR-V7 to AR-FL. [1,2] Additional details are provided below.

Blood samples were collected using standard BD Vacutainer® lavender top blood collection tubes (Becton Dickinson, Franklin Lakes, NJ) (Product #: 367862) by venipuncture, and carried to the lab on ice. Laboratory processing was carried out within 2 hours of collection, according to instructions provided by the Alere™ CTC AdnaTest (Alere Inc., San Diego, CA). The AdnaTest is a CE-marked, RNA-based CTC enrichment and detection test with two components/kits. Briefly, the ProstateCancerSelect (Product No. T-1-520) kit was used to enrich CTC from 5ml blood using magnetic particles coated with a combination of antibodies recognizing prostate cancer cells, while the ProstateCancerDetect (Product No. T-1-521) kit was used to make cDNA for detection of prostate cancer-associated RNA transcripts using multiplexed polymerase chain reaction (PCR). On the basis of detection of PCR signals for PSA, PSMA, or EGFR (very rarely detected) by the Agilent Bioanalyzer (Agilent Technologies, Palo Alto, CA), CTC calls were made for each sample tested. The test was adapted for detection and quantification of AR-FL and AR-V7 by quantitative real-time PCR using custom primers specific for AR-FL (forward: 5'-CAGCCTATTGCGAGAGAGCTG-3', reverse: 5'-GAAAGGATCTTGGGCACTTGC-3') and AR-V7 (forward: 5'-CCATCTTGTCGTCTTCGGAAATGTTA-3', reverse: 5'-TTTGAATGAGGCAAGTCAGCCTTTCT-3'). Briefly, PCR reactions were carried out under optimized conditions at 95°C x 10s, 58°C x 30s, and 72°C x 30s for 39 cycles followed by melting curve analysis.

Standard dilution curves from known quantities of AR-FL and AR-V7 was generated for calculating absolute transcript copy numbers for AR-FL and AR-V7. Laboratory data was generated for each patient enrolled in the study in a blinded fashion and recorded into the master data sheet on a weekly basis. To rule out false positive and false negative findings, a number of quality control measures were implemented each time the assay was performed, including negative and positive controls at multiple levels for both CTC detection and AR quantification. This laboratory-developed RNA-based assay modified from a commercially available circulating tumor cell (CTC) detection platform was thoroughly evaluated and internally validated with standard quality measures implemented. First, all samples collected from healthy volunteers (n=4) and CTC-negative CRPC patients (n=9) were negative for AR-FL and AR-V7, excluding the possibility of false-positive detection due to contaminating leukocytes. Second, the test consistently detected both AR-FL and AR-V7 in normal blood samples spiked with 5 AR-V7 positive cells (n=6). Third, overnight shipping of blood samples and storage of partially processed cell lysates (up to two weeks) did not compromise assay results (although our current study does not involving shipping). Fourth, all tests on clinical specimens were performed using a fraction (10%) of the cDNA yield from 5 mL of blood, and were always accompanied by two negative and two positive controls. Detailed technical protocols will be made available upon request.

RNA *in situ* hybridization

RNA in situ hybridization (RISH) was performed to detect the androgen receptor (AR) and AR-V7 using the ACD (Advanced cell Diagnostics, Hayward, CA) RNAscope 2.0 Brown kit. Briefly, formalin-fixed paraffin-embedded (FFPE) tissue or cell pellet blocks were sectioned and the slides baked for one hour at 60^0C. The slide were subsequently de-paraffinized with xylene for 20 min at room temperature, and allowed to air dry following two rinses using 100% ethanol. Following a series of pretreatment steps, the cells were permeablized using protease to allow probe access to the RNA target. ACD target probes, a series of paired oligonucleotides forming a binding site for a preamplifier, were custom designed to detect RNA corresponding to exon 1 of the human AR (ACD 401211), or the cryptic AR exon 3 sequence [1,3] that encode human AR-V7 (ACD 401221). Hybridization of the probes to the AR

RNA targets was performed by incubation in the oven for 2 hours at 40 ^{0}C. Following two washes, the slides were processed for standard signal amplification steps per manufacturer's instructions.

Western Blot

Whole cell protein extracts were prepared from cultured prostate cancer cells or cryosections prepared from clinical specimens by using RIPA buffer (radioimmunoprecipitation assay buffer) (Cell Signaling Technology, Danvers, MA) supplemented with 1X protease inhibitors (Roche, Indianapolis, IN) and 1X phosphatase inhibitors (Thermo Fisher Scientific, Rockford, IL). Standard blots were prepared following electrophoresis of forty μg protein per sample on a 10% SDS-PAGE precast gel (Bio-Rad Laboratories, Hercules, CA), and incubated overnight with anti-AR-V7 [4] (1 μg/mL), anti-AR (N20) (1:2000 dilution) (sc-816, Santa Cruz Biotechnology, Dallas, TX), anti-PSA (C-19) (1:500) (sc-7638, Santa Cruz Biotechnology), and anti-β-actin (1:5000 dilution) (Sigma, St Louis, MO). Following incubation with horseradish-peroxidase(HRP)-conjugated secondary antibodies, immunoreactive bands were visualized using the SuperSignal West Pico Chemiluminescent Substrate system (I-34080) (Thermo Fisher Scientific, Rockford, IL) on HyBlot CL film (E3022) (Denville Scientific, South Plainfield, NJ).

Prostate cancer cell lines

LNCaP cells (ATCC, Manassas, VA) were maintained in RPMI1640 medium (Invitrogen, Carlsbad, CA) with 10% fetal bovine serum (FBS, Sigma–Aldrich, St. Louis, MO). LNCaP95 is an AR-V7-positive androgen-independent cell line derived from the parental LNCaP cells as described previously [4]. LNCaP95 cells were maintained in phenol red-free RPMI 1640 medium supplemented with 10% charcoal stripped FBS (CSS). For analysis of androgen-induced changes in AR-V7, LNCaP95 cells were treated with R1881 (NEN, Waltham, MA) or ethanol vehicle control as described previously [4]. These cell lines were authenticated (DDC Medical, Fairfield, OH) using short tandem repeats DNA profiling and tested negative for mycoplasma.

Metastatic prostate tumor tissue specimens

To investigate concordance in AR-V7 status between CTCs and tumor tissue, qRT-PCR analysis for AR-V7 was performed on fresh metastatic tumor biopsies (or autopsy specimens) from a subset of patients who consented to this. In addition, RNA in situ hybridization (RNA-ISH) was performed according to the manufacturer's instructions using the RNAscope platform (Advanced Cell Diagnostics, Hayward, CA) to visualize AR-V7 mRNA in formalin-fixed paraffin-embedded metastatic tumor tissues, and to correlate this with AR-V7 detection in CTCs. Additional details are provided below.

Research autopsies were performed on two patients who died during the course of treatment with enzalutamide. Both patients were AR-V7 positive as determined by the CTC assay before and after treatment. Metastatic prostate tumors were dissected and flash frozen blocks prepared. Following histological analysis, cryosections enriched for tumor cells were prepared following manual trimming of the frozen blocks, using a standard procedure as described previously [5]. High-quality total RNA in adequate quantity was extracted from two specimens (one from each patient) and labeled as AR-V7(+) Met1 and AR-V7(+) Met2, respectively. To identify relevant AR-V7-negative metastatic CRPC samples for comparison, we analyzed AR-FL and AR-V7 expression levels in a separate collection of CRPC specimens from men consented for autopsy (before the development of enzalutamide and abiraterone) as described previously [1,6,7]. Two specimens that were AR-V7 negative but with AR-FL levels similar to those detected in other mCRPC specimens were identified from this collection of specimens. These two samples were labeled AR-V7(-) Met1 and AR-V7(-) Met2. Both samples were processed histologically in a similar fashion to enrich prostate carcinoma cells.

RNA-Seq analysis

Four metastatic prostate tissue specimens, AR-V7(+) Met1, AR-V7(+) Met2, AR-V7(-) Met1, and AR-V7(-) Met 2, were subjected to RNA-Seq following the standard TruSeq Stranded Total RNA Sample Prep Kit and sequenced using the Illumina HiSeq 2000 platform (Illumina Inc, San Diego, CA). We generated an average of ~63 million reads per sample. Sequences were aligned to UCSC hg19 genome build using TopHat, and mutation and splice junctions visualized using Integrated Genome

Viewer (IGV) [8]. Read counts (gene expression levels) were obtained using HTSeq [9], and normalized per kilo base-pair gene length and per million reads library size (RPKM). Fold expression changes (FC) between the two conditions (AR-V7(+) and AR-V7(-)) were calculated. Genes were pre-ranked by logFC and subjected to Gene Set Enrichment Analysis (GSEA) [10]. Both raw and processed RNA-Seq data were deposited in the Gene Expression Omnibus (accession number: GSE56701).

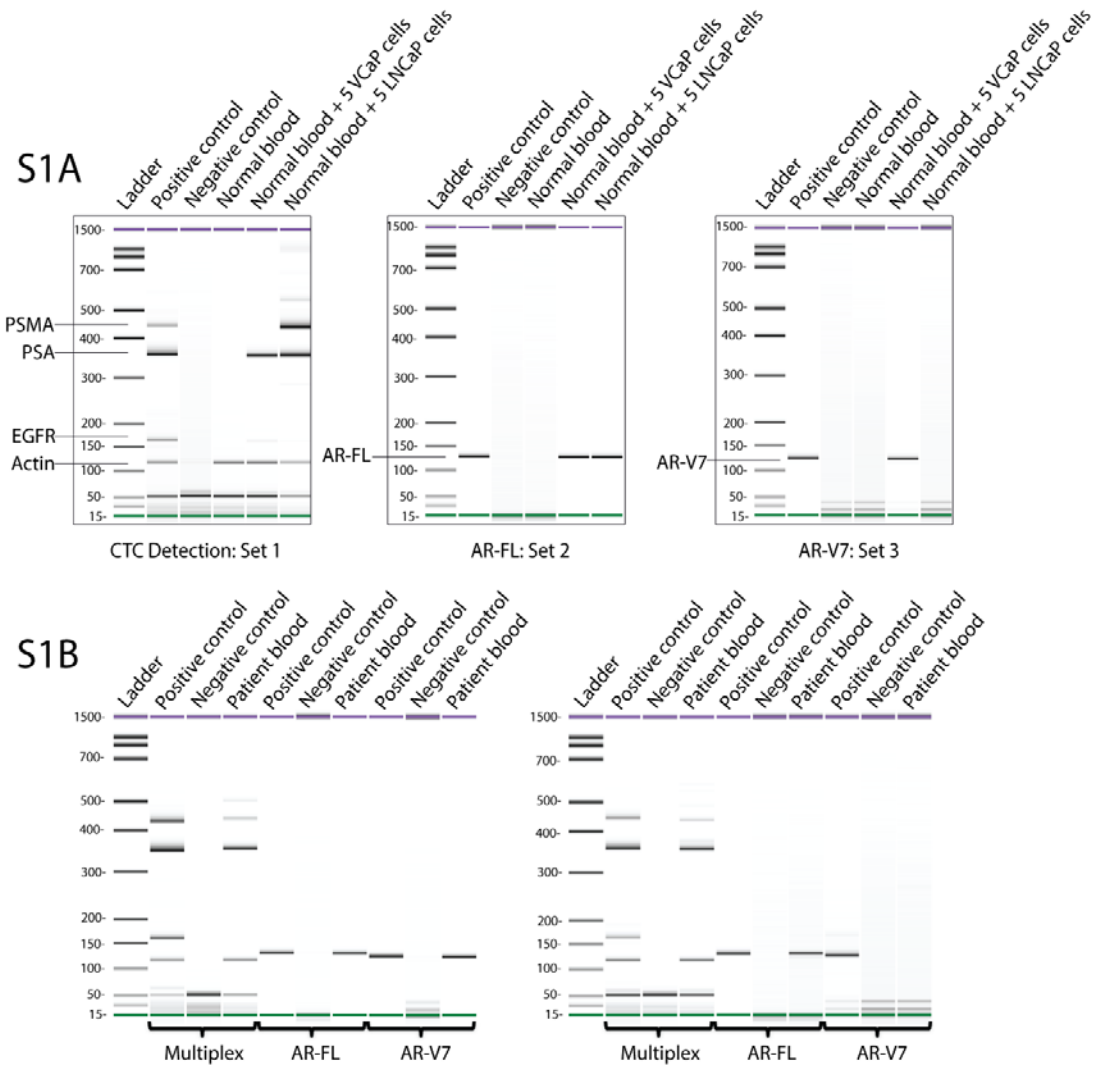

Figure S1. Detection of AR-V7 transcript in CTCs.

(A) Blood-based detection of full-length androgen receptor (AR-FL) and AR splice variant-7 (AR-V7) transcripts in tumor cells spiked into 5 mL of blood from normal human volunteers. Following CTC capture, lysis, and cDNA synthesis, three sets of independent PCR reactions were performed to examine the presence of CTC-specific mRNA transcripts by multiplex PCR (set 1), as well as transcripts for AR-FL (set 2) and AR-V7 (set 3). **(B)** Examples of positive and negative detection of AR-V7 in baseline (pre-treatment) blood samples from two enzalutamide-treated patients. The patient in the **left panel** is positive for both AR-FL and AR-V7, while the patient in the **right panel** is positive only for AR-FL but negative for AR-V7. Both patients were positive for CTCs, as determined by the multiplex PCR assay (based on the examination of PSMA, PSA, EGFR and Actin) per the manufacturer's instructions provided by AdnaGen.

S2 A

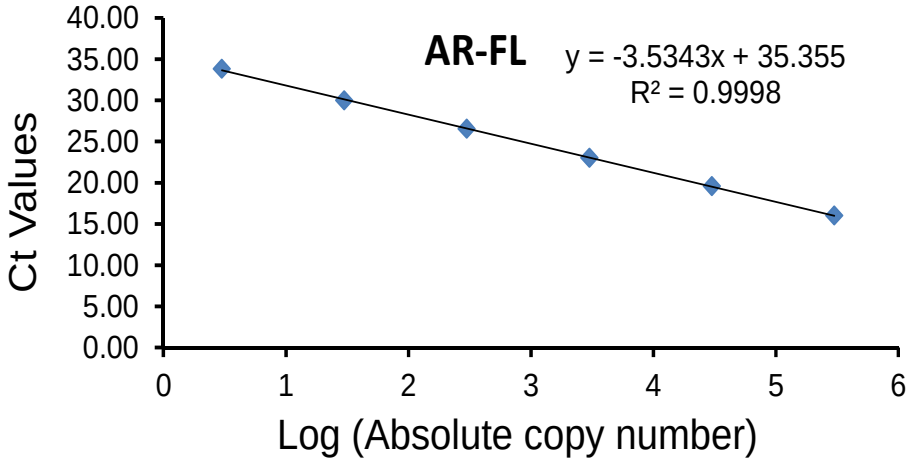

S2 B

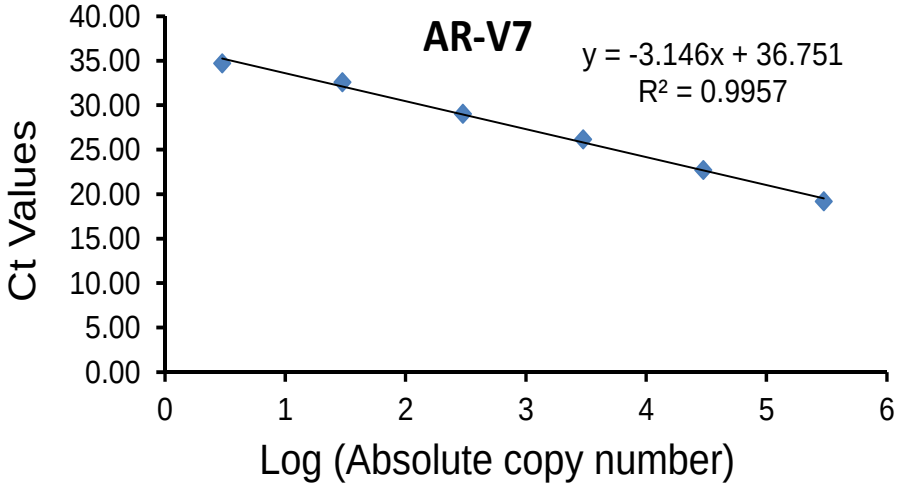

Figure S2. Justification for threshold of detection of AR-V7.

Standard dilution curves for AR-FL and AR-V7 are shown. Threshold cycle numbers (Y axis) in quantitative PCR reactions were determined for complementary DNA (cDNA) specific to AR-FL **(A)** and AR-V7 **(B)** at 6 dilutions containing the indicated number of copies of each transcript (X axis). Formulas were derived to quantify the absolute copy numbers on the basis of Ct values.

S3 A

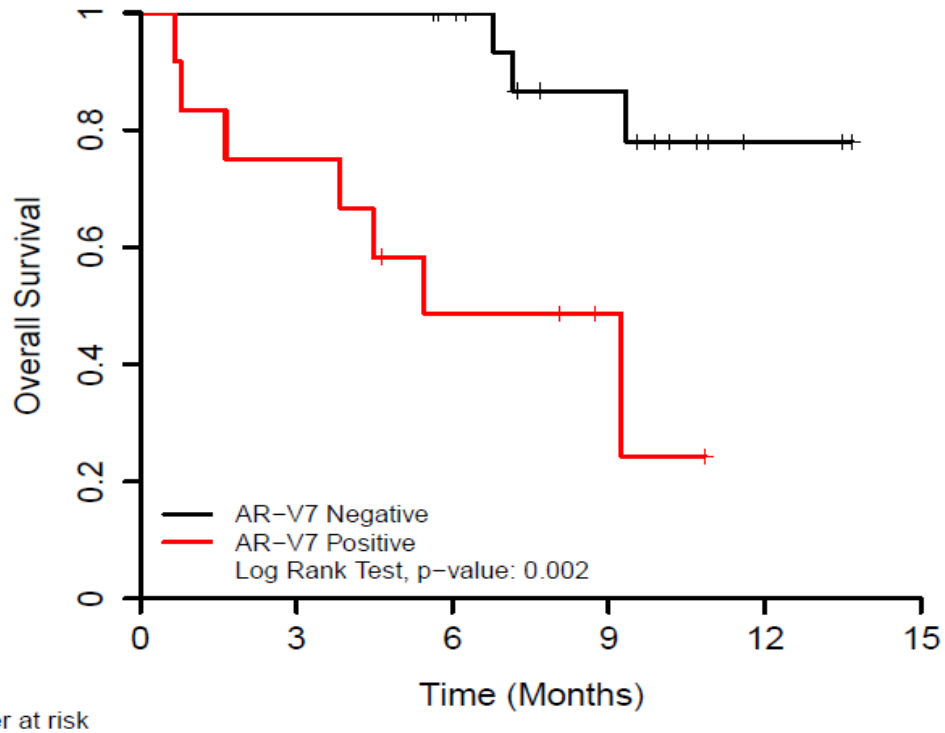

Number at risk						
AR−V7 Negative:	19	19	17	10	2	0
AR−V7 Positive:	12	9	5	2	0	0

S3 B

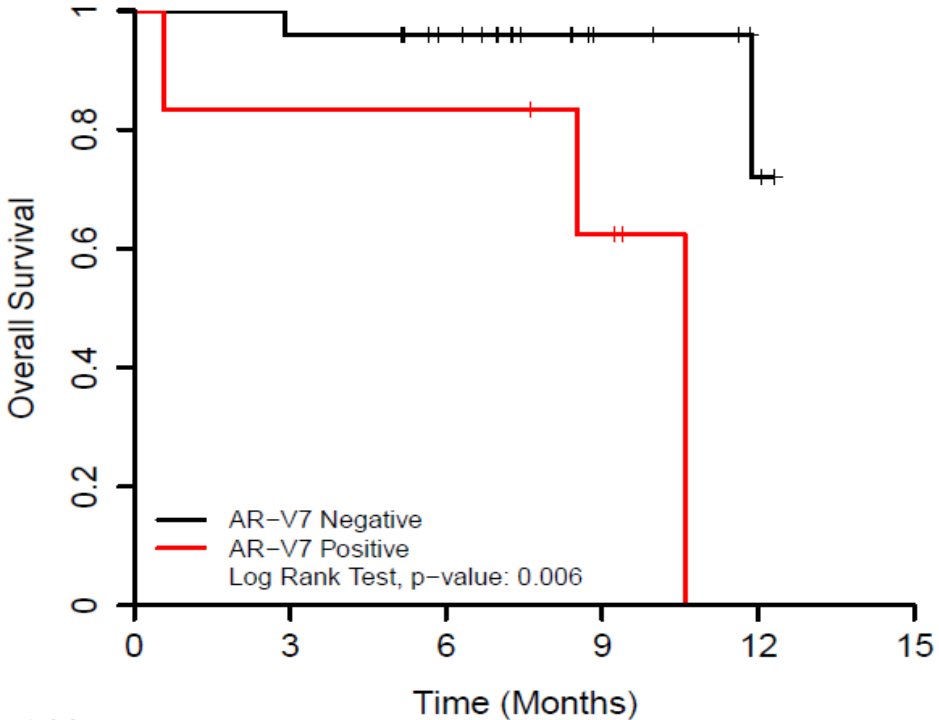

Number at risk						
AR−V7 Negative:	25	24	19	7	3	0
AR−V7 Positive:	6	5	5	3	0	0

Figure S3. Overall survival (OS) analysis stratified by AR-V7 status in enzalutamide-treated patients and abiraterone-treated patients.

(A) Median OS in enzalutamide-treated patients was 5.5 months (95%CI, 3.9–not reached) and not reached (95%CI, not reached–not reached) in AR-V7–positive and AR-V7–negative patients, respectively (HR 6.9, 95%CI 1.7–28.1, log-rank *P*=0.002).

(B) Median OS in abiraterone-treated patients was 10.6 months (95%CI, 8.5–not reached) and >11.9 months (95%CI, 11.9–not reached) in AR-V7–positive and AR-V7–negative patients, respectively (HR 12.7, 95%CI 1.3–125.3, log-rank *P*=0.006).

S4 A

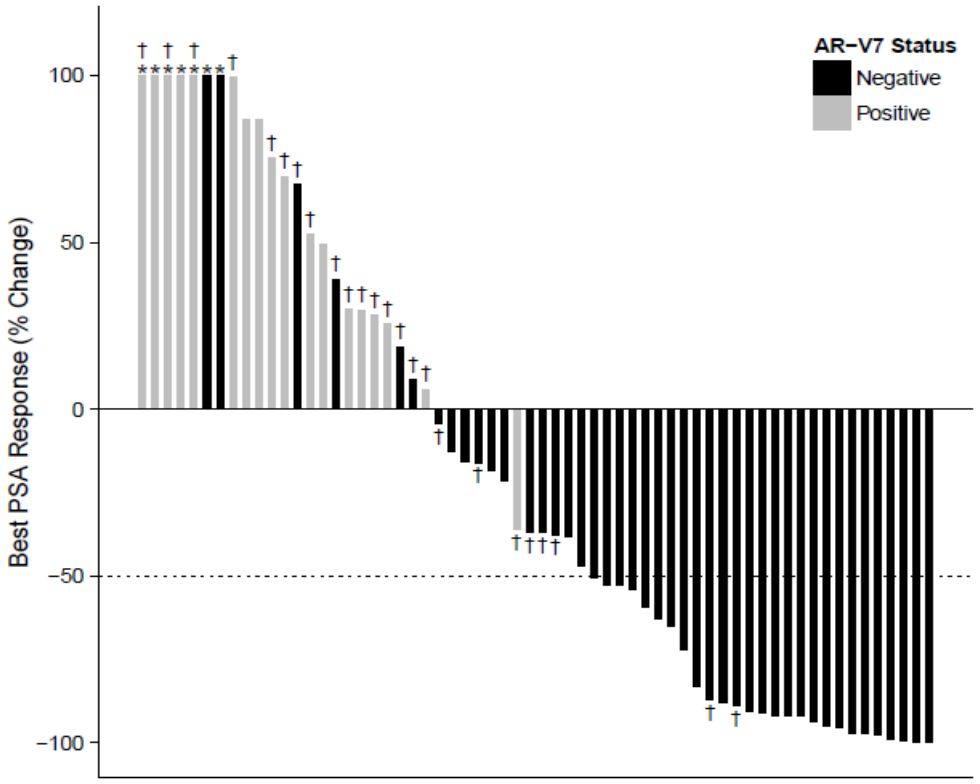

S4 B

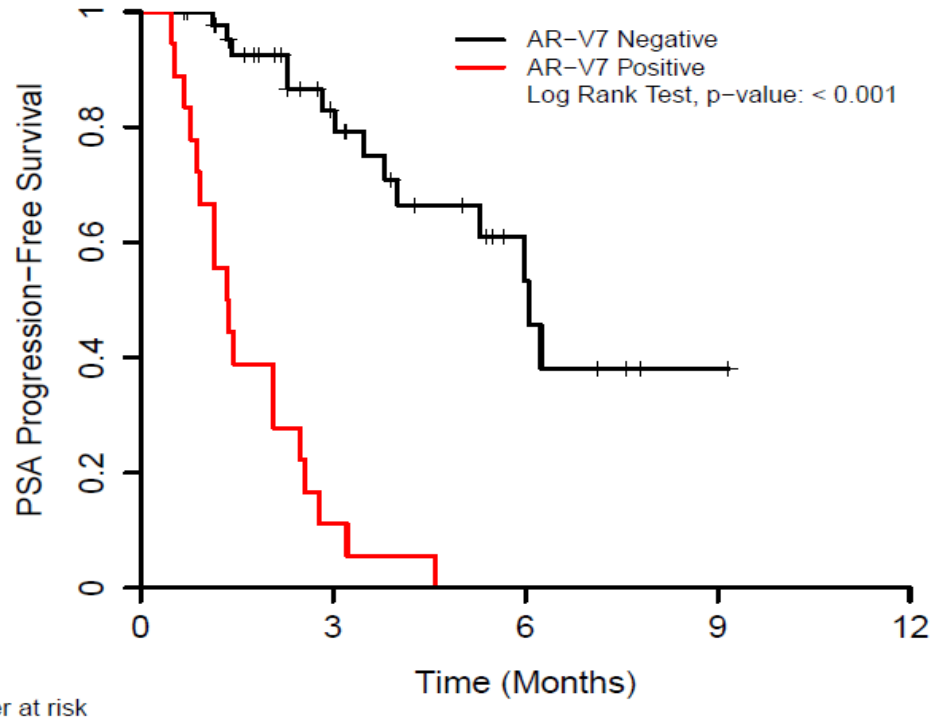

Number at risk

AR−V7 Negative:	44	22	7	1	0
AR−V7 Positive:	18	2	0	0	0

S4 C

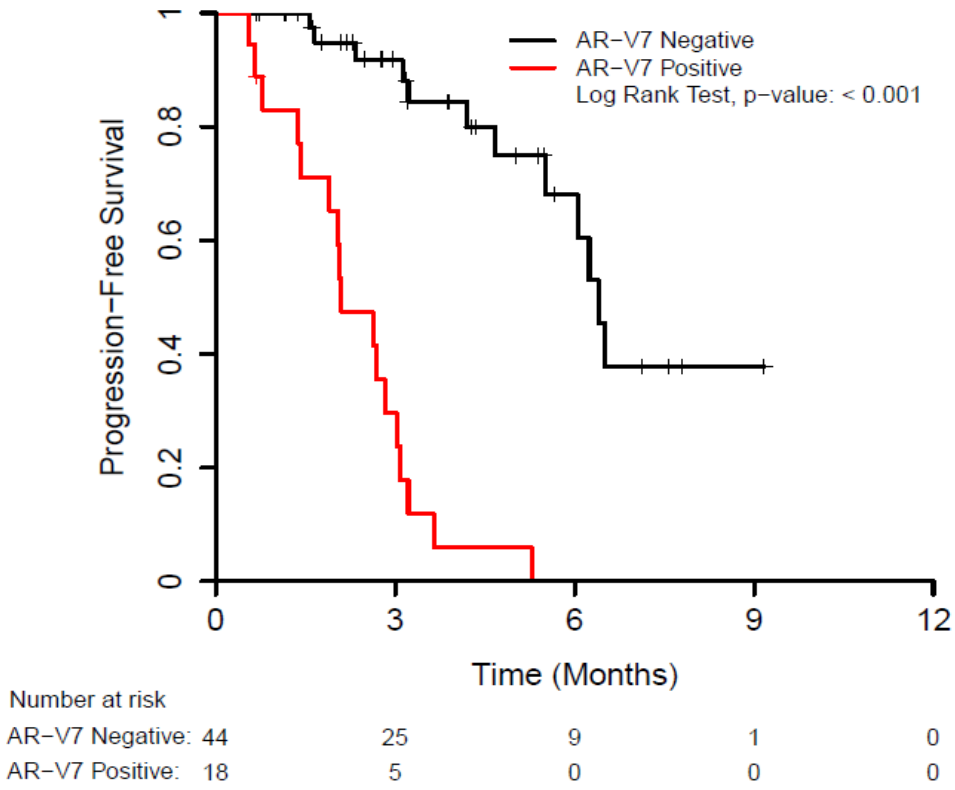

Number at risk					
AR−V7 Negative:	44	25	9	1	0
AR−V7 Positive:	18	5	0	0	0

S4 D

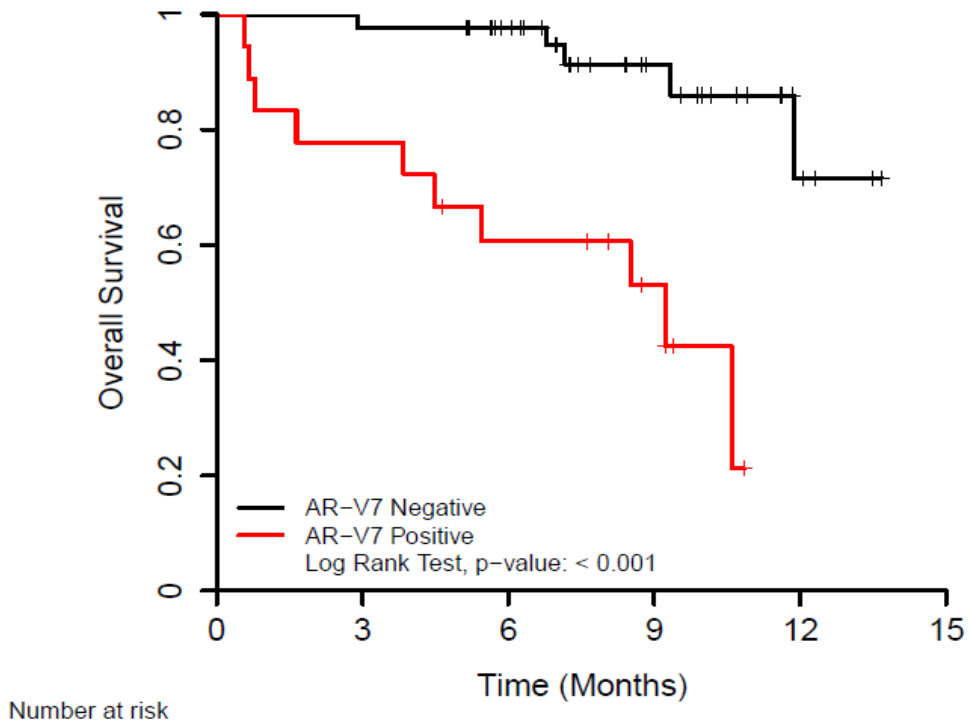

Number at risk						
AR−V7 Negative:	44	43	36	17	5	0
AR−V7 Positive:	18	14	10	5	0	0

Figure S4. Combined analysis of patient outcome by AR-V7 status.

(A) Waterfall plot showing best PSA responses according to CTC AR-V7 status for all 62 patients. The 'asterisk' marks (*) indicate clipped bars. The dotted line shows the threshold for defining a PSA response. Men who had previously received abiraterone and enzalutamide (in the enzalutamide and abiraterone cohorts, respectively) are denoted with 'dagger' marks (†). The overall proportion of patients who achieved a PSA response to either therapy was 44% (27/62 men; 95%CI, 31–57%). PSA response rates were 0% (0/18 men; 95%CI, 0–19%) in AR-V7–positive patients and 61% (27/44 men; 95%CI, 45–76%) in AR-V7–negative patients (P<0.001). Considered alternatively, among patients achieving a PSA response, 0% (0/27 men; 95%CI, 0–13%) were AR-V7–positive; while in patients not achieving a PSA response, 51% (18/35 men; 95%CI, 34–69%) were AR-V7–positive. In linear regression modeling, AR-V7 status remained predictive for PSA response after adjusting for AR-FL expression levels (P<0.001). **(B) Kaplan-Meier curves showing PSA-progression-free-survival [PSA-PFS] stratified by CTC AR-V7 status in all 62 patients.** Median PSA-PFS was 1.4 months (95%CI, 0.9–2.6) and 6.1 months (95%CI, 5.3–not reached) in AR-V7–positive and AR-V7–negative patients, respectively (HR 10.5, 95%CI 4.7–23.6, log-rank P<0.001). In multivariable Cox regression analysis stratified by treatment type, AR-V7 detection remained independently predictive of PSA-PFS (HR 8.2, 95%CI 2.7–24.9, P<0.001). Presence of visceral metastases and more prior hormonal therapies were also predictive of PSA-PFS; while AR-FL level, prior use of enzalutamide/abiraterone, and baseline PSA level were not predictive. **(C) Kaplan-Meier curves showing clinical/radiographic-progression-free-survival [PFS] stratified by CTC AR-V7 status in all 62 patients.** Median PFS was 2.1 months (95%CI, 1.9–3.1) and 6.4 months (95%CI, 6.1–not reached) in AR-V7–positive and AR-V7–negative patients, respectively (HR 12.7, 95%CI 5.1–31.9, log-rank P<0.001). In multivariable Cox regression analysis stratified by treatment type, AR-V7 detection remained independently predictive of PFS (HR 4.9, 95%CI 1.7–13.8, P=0.003). AR-FL levels, more prior hormonal therapies and prior use of enzalutamide/abiraterone were also predictive of PFS; while baseline PSA level, and presence of visceral metastases were not predictive. **(D) Kaplan-Meier curves showing overall survival [OS] stratified by CTC AR-V7 status in all 62 patients.** Median OS was 9.2 months (95%CI, 4.5–not reached) and >11.9 months (95%CI, 11.9–not reached) in AR-V7–positive and AR-V7–negative patients, respectively (HR 8.3, 95%CI 2.5–27.4, log-rank P<0.001). In multivariable Cox regression analysis stratified by treatment type, AR-V7 detection remained independently predictive of OS (HR 5.0, 95%CI 1.3–19.8, P=0.021). Prior use of enzalutamide/abiraterone was also predictive of OS, while AR-FL level was not predictive.

S5 A

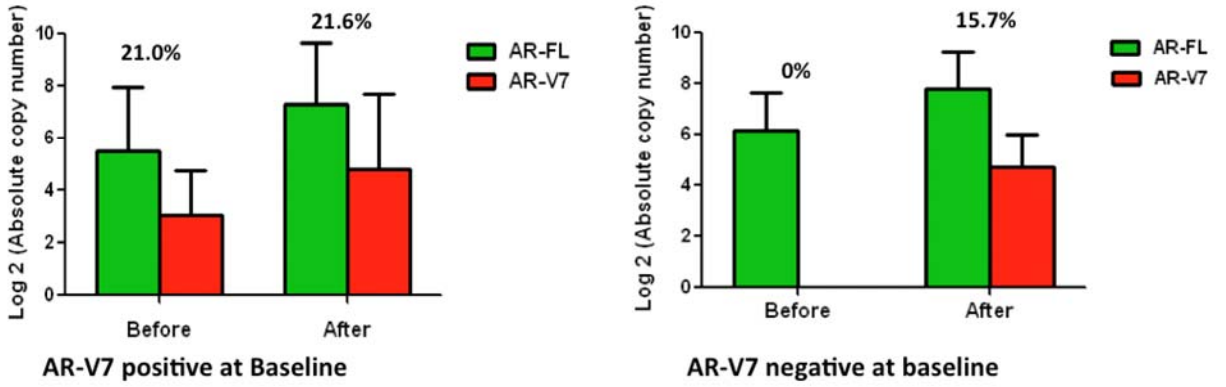
Log 2 (Absolute copy number)
21.0%
21.6%
AR-FL
AR-V7
Before
After
AR-V7 positive at Baseline
0%
15.7%
AR-V7 negative at baseline

S5 B

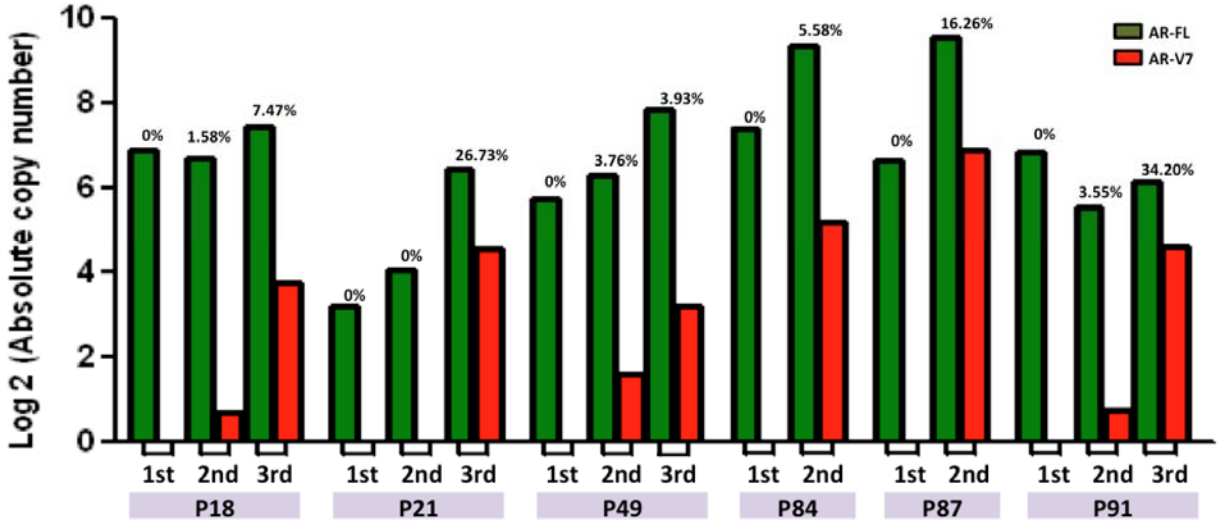
Log 2 (Absolute copy number)
AR-FL
AR-V7
0%
1.58%
7.47%
0%
0%
26.73%
0%
3.76%
3.93%
0%
5.58%
0%
16.26%
0%
3.55%
34.20%
1st 2nd 3rd
P18
P21
P49
P84
P87
P91

Figure S5. Changes in AR-V7 and AR-FL transcript copy numbers detected in CTCs before and after treatment with enzalutamide and abiraterone.

(A) Alterations in AR-FL and AR-V7 transcript copy numbers before and after enzalutamide/abiraterone treatment in patients with baseline detectable AR-V7 (n=16, with paired samples available) (*left* panel) and in patients who converted from initially undetectable to later detectable AR-V7 (n=6) (*right* panel). Higher copy numbers for both AR-FL and AR-V7 were detected in CTC samples collected after treatment (at the time of resistance to therapy) compared to baseline (pretreatment) samples. Note that the AR-V7/AR-FL ratio is similar between samples collected before and after treatment in patients with baseline detectable AR-V7 (~21%), and that an average AR-V7/AR-FL ratio of 15.7% was detected in patients who converted from initially undetectable to later detectable AR-V7. In patients who converted from initially undetectable to later detectable AR-V7, copy number values for AR-V7 were generated from the last follow-up CTC samples (see B, below).

(B) AR transcript copy numbers detected in the 6 patients whose AR-V7 status was negative at baseline but converted to positive during treatment. Absolute transcript copy numbers for AR-FL and AR-V7 are shown for each of the 6 patients before, during, and after treatment with enzalutamide or abiraterone (1st: before treatment; 2nd: during treatment; 3rd: at the time of progression). The percentage values represent the ratio of the absolute copy number of AR-V7 to AR-FL in CTCs. As shown, absolute AR-V7 levels (and AR-V7/AR-FL ratios) increased with time in all 6 cases. Patients P18, P21, P49 and P87 were treated with enzalutamide. Patients P84 and P91 were treated with abiraterone.

S6

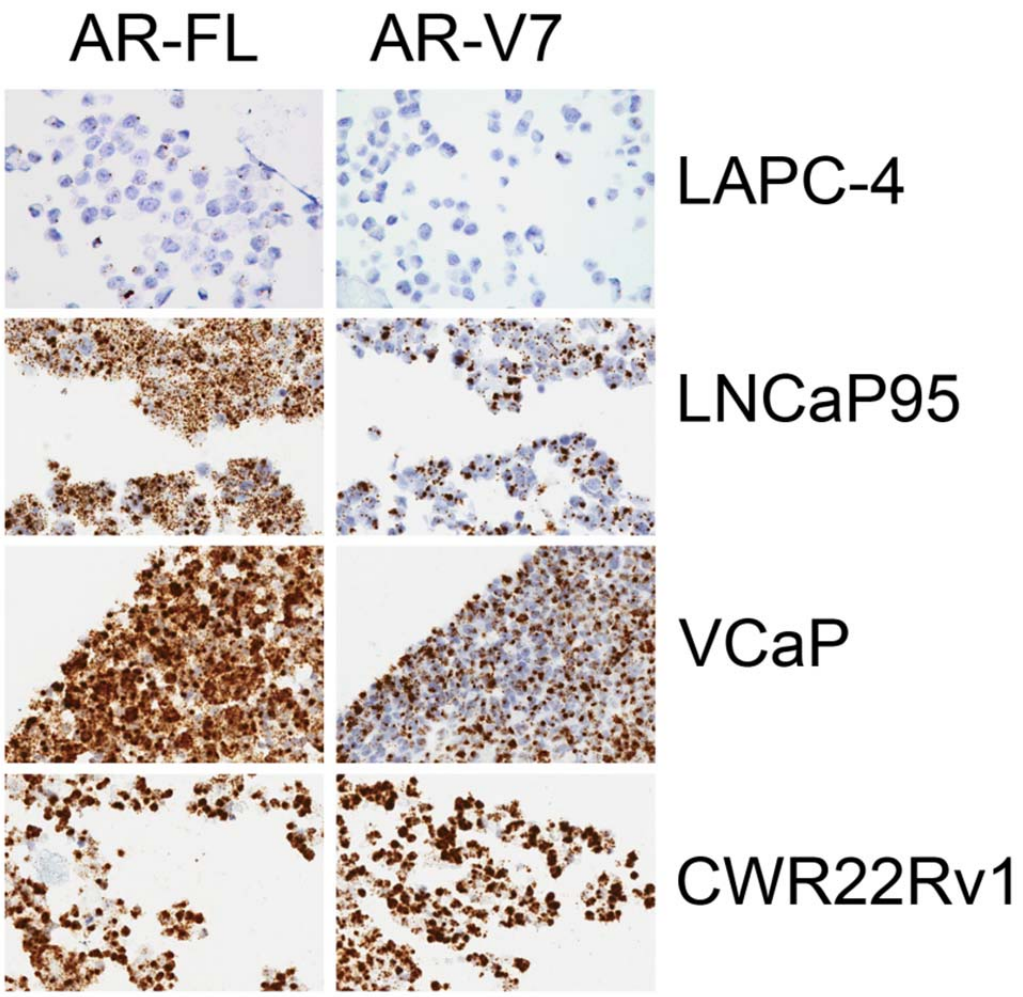

Figure S6. Detection of AR-FL and AR-V7 using RNA-ISH in cell lines with known expression of AR-FL and AR-V7.

Three of the prostate cancer cell lines shown (LNCaP95, VCaP and CWR22Rv1) express AR-FL as well as AR-V7, while the LAPC-4 line is positive only for AR-FL but negative for AR-V7, as visualized using RNA-ISH analysis. These prostate cancer cell lines served as positive and negative controls for AR-V7 detection by RNA-ISH in the patient-derived metastatic prostate cancer tissue samples shown in Fig. 4 of the main manuscript.

S7

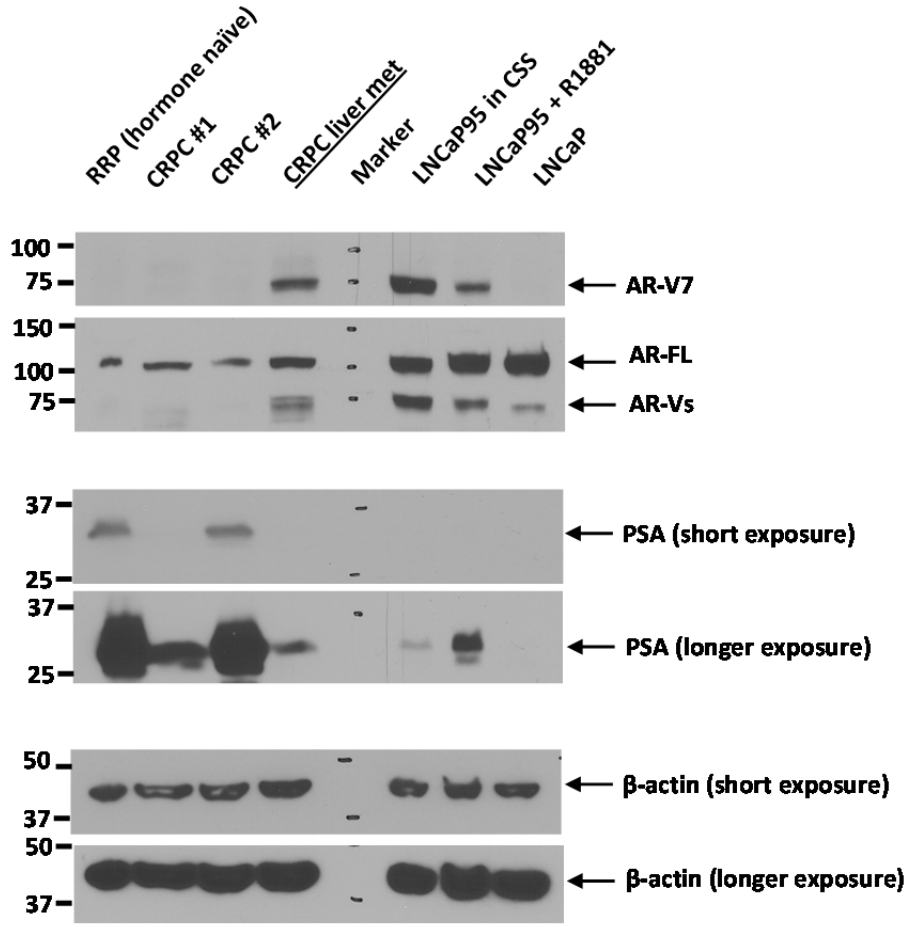

Figure S7. Detection of AR-V7 at the protein level using Western blot analysis in patients with detectable AR-V7 transcript in CTCs.

Detection of AR-V7 protein expression in a representative tissue sample, in this case from a liver metastasis from an AR-V7–positive patient (underlined label). Whole protein extractions were prepared from cryosections using RIPA buffer with protease inhibitors and phosphatase inhibitors. 40 μg of protein from each sample was separated on a 10% SDS-PAGE precast gel and blotted with anti–AR-V7, anti–AR (N20) (for detection of both AR-FL and AR-Vs), anti-PSA, and anti–β-actin antibodies. The LNCaP cell line served as the negative control for AR-V7; the LNCaP95 cell line (in the presence or absence of synthetic androgen, R1881) served as the positive control for AR-V7. Also shown for comparison are samples from a hormone-naïve radical prostatectomy specimen (RRP), and two metastatic tissue samples from AR-V7–negative patients (CRPC #1 and CRPC #2). Molecular weight marks are indicated to the left of the blots.

S8

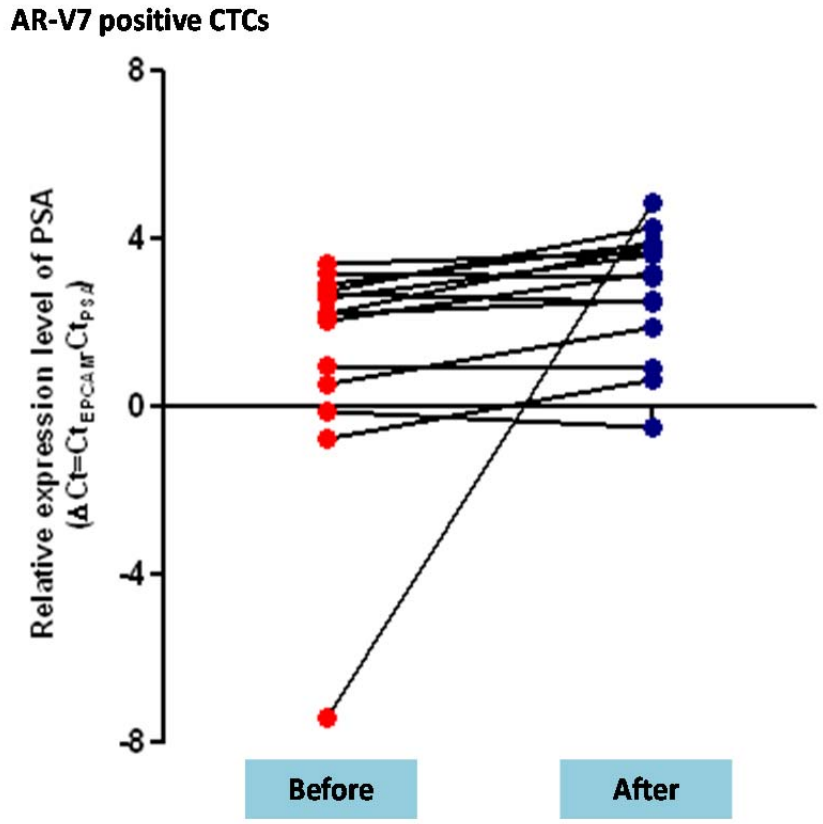

Figure S8. Changes in expression levels of the PSA transcript before and after therapy with enzalutamide or abiraterone in men with baseline detectable AR-V7.

PSA expression changes in CTC samples from AR-V7–positive patients before and after treatment with enzalutamide/abiraterone (n=14), as assessed by qRT-PCR. Results are shown as the difference in Ct value between EPCAM and PSA expression ($Ct_{EPCAM} - Ct_{PSA}$). As depicted, PSA expression was generally increased during treatment with enzalutamide/abiraterone in AR-V7–positive patients, suggesting that canonical AR signaling (as indicated by levels of PSA mRNA normalized to those of EPCAM) was not inhibited by enzalutamide/abiraterone in the presence of AR-V7.

S9

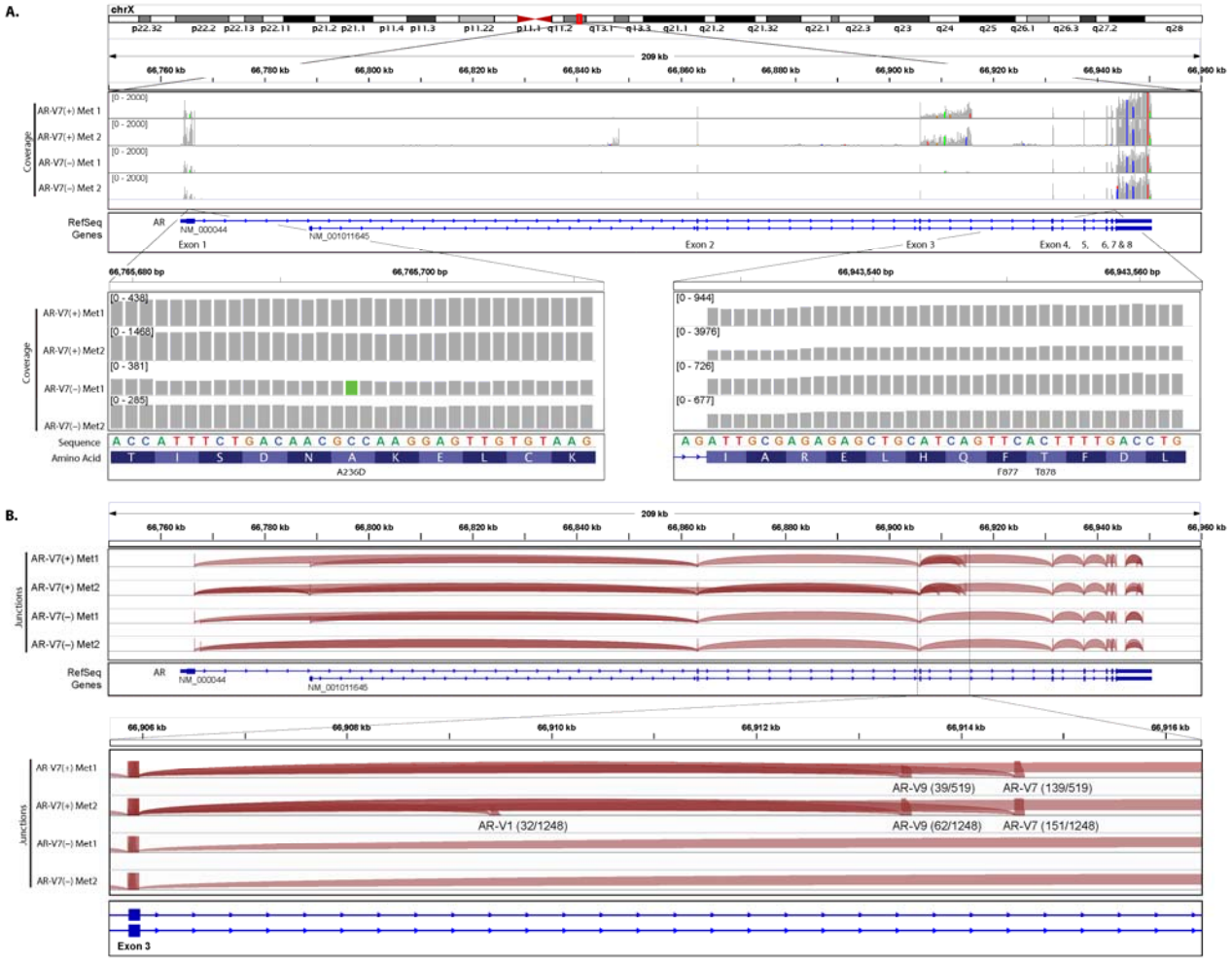

Figure S9. RNA-Seq analysis of the AR transcript in two AR-V7 (+) and two AR-V7 (–) patients.

(**A**) Read coverage along the AR gene, with the enlarged view showing a novel AR mutation (A236D) in exon 1 (of unknown significance) detected in an AR-V7-negative tumor, but a lack of known AR ligand-binding domain (LBD) mutations F876L and T877A previously implicated in castration resistance and enzalutamide resistance (note: due to Refseq sequence changes, the numbering of amino acid positions have increased by one). A236D is the only AR mutation detected in these four samples. **(B)** AR RNA splice junction tracks depicting sequence reads connecting canonical and cryptic AR exons (junctions supported by a read depth of at least 20 are shown in the figure). The enlarged region spanning exon 3 and intron 3 shows positively identified AR-V7 variants (along with AR-V1 and AR-V9) in the tissue samples from the two AR-V7–positive patients. Numbers in parentheses indicate the number of variant-specific reads over the number of AR-FL–specific reads. The AR-V7/AR-FL ratios were 26.8% and 12.1%, for AR-V7(+) Met1 and AR-V7(+) Met2, respectively.

S10

Positive enrichment in prostate related gene sets

Gene Set Details	# of genes	ES	NES	Norm p-val	FDR q-val
1. RESPONSE_TO_WOUNDING	87	0.64	2.27	0	0
2. DEFENSE_RESPONSE	105	0.61	2.18	0	0
3. CELLULAR_DEFENSE_RESPONSE	16	0.86	2.18	0	0
4. RESPONSE_TO_EXTERNAL_STIMULUS	135	0.57	2.16	0	0
5. INFLAMMATORY_RESPONSE	60	0.63	2.12	0	0
6. M_PHASE_OF_MITOTIC_CELL_CYCLE	67	0.61	2.08	0	0
7. G_PROTEIN_COUPLED_RECEPTOR_PROTEIN_SIGNALING_PATHWAY	83	0.59	2.06	0	0.001
8. MITOSIS	64	0.6	2.02	0	0.002
9. M_PHASE	81	0.57	1.97	0	0.003
10. ORGAN_MORPHOGENESIS	79	0.56	1.96	0	0.003

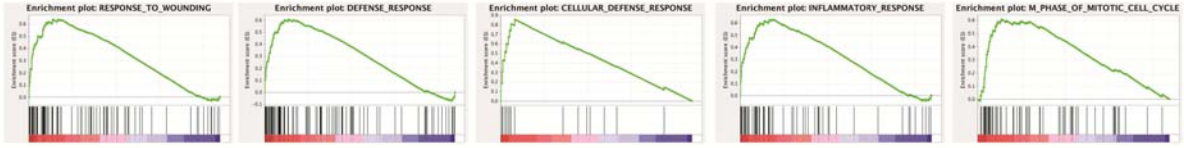

Negative enrichment in prostate related gene sets

Gene Set Details	# of genes	ES	NES	Norm p-val	FDR q-val
1. GOLGI_VESICLE_TRANSPORT	47	-0.38	-1.49	0.033	1
2. CHROMATIN_ASSEMBLY_OR_DISASSEMBLY	22	-0.43	-1.33	0.115	1
3. GAMETE_GENERATION	44	-0.34	-1.27	0.114	1
4. MRNA_PROCESSING_GO_0006397	70	-0.28	-1.17	0.135	1
5. ER_TO_GOLGI_VESICLE_MEDIATED_TRANSPORT	18	-0.39	-1.16	0.223	1
6. NEGATIVE_REGULATION_OF_TRANSCRIPTION_DNA_DEPENDENT	94	-0.25	-1.12	0.184	1
7. MRNA_METABOLIC_PROCESS	81	-0.26	-1.11	0.194	1
8. NEGATIVE_REGULATION_OF_RNA_METABOLIC_PROCESS	95	-0.26	-1.1	0.259	1
9. SEXUAL_REPRODUCTION	50	-0.28	-1.1	0.288	1
10. PROTEIN_AUTOPROCESSING	22	-0.34	-1.1	0.303	1

Figure S10. Gene set enrichment analysis of metastatic tumors from AR-V7–positive and AR-V7–negative patients.

Top ranked 'biological processes' enriched in genes differentially expressed between AR-V7–positive and AR-V7–negative metastatic prostate cancer tissues are shown. Genes are pre-ranked based on fold expression changes. Consistent with the 'AR-V7 up' and 'AR-FL up' gene signatures reported in our previous study,[4] cell cycle genes previously shown to be driven by AR-V7 (*i.e.*, 'AR-V7 up') are enriched for increased expression in AR-V7–positive samples, and genes involved in Golgi activities, previously linked to AR-FL activity (*i.e.*, 'AR-FL up'), are downregulated in AR-V7-positive samples.
[ES: enrichment score. NES: normalized enrichment score].

Table S1 A. Baseline characteristics of the 31 patients treated with enzalutamide.

Baseline Characteristic	All Patients (N=31)	AR-V7 Negative (N=19)	AR-V7 Positive (N=12)	P-value*
Age (years)				
median (range)	70 (56–84)	72 (60–84)	69 (56–82)	0.223
Race, N (%)				
white	26 (83.9%)	16 (84.2%)	10 (83.3%)	
non-white	5 (16.1%)	3 (15.8%)	2 (16.7%)	0.999
Time since diagnosis (years)				
median (range)	5 (1–21)	5 (1–21)	7 (1–18)	0.760
Tumor stage at diagnosis, N (%)				
T1/T2	17 (54.8%)	10 (52.6%)	7 (58.3%)	
T3/T4	14 (45.2%)	9 (47.4%)	5 (41.7%)	0.999
Gleason sum at diagnosis, N (%)				
≤7	12 (40.0%)	9 (47.4%)	3 (27.3%)	
≥8	18 (60.0%)	10 (52.6%)	8 (72.7%)	0.442
Type of local treatment, N (%)				
surgery	13 (41.9%)	8 (42.1%)	5 (41.7%)	
radiation	7 (22.6%)	6 (31.6%)	1 (8.3%)	
none	11 (35.5%)	5 (26.3%)	6 (50.0%)	0.262
Number of prior hormonal therapies				
mean (range)	3.3 (2–5)	3.2 (2–5)	3.4 (3–5)	0.317
Prior use of abiraterone, N (%)				
yes	20 (64.5%)	9 (47.4%)	11 (91.7%)	
no	11 (35.5%)	10 (52.6%)	1 (8.3%)	0.020
Prior use of docetaxel, N (%)				
yes	20 (64.5%)	10 (52.6%)	10 (83.3%)	
no	11 (35.5%)	9 (47.4%)	2 (16.7%)	0.128
Presence of bone metastases, N (%)				
yes	28 (90.3%)	17 (89.5%)	11 (91.7%)	
no	3 (9.7%)	2 (10.5%)	1 (8.3%)	0.999
Number of bone metastases, N (%)				
≤5	20 (64.5%)	15 (78.9%)	5 (41.7%)	
≥6	11 (35.5%)	4 (21.1%)	7 (58.3%)	0.056
Presence of visceral metastases, N (%)				
yes	10 (32.3%)	3 (15.8%)	7 (58.3%)	
no	21 (67.7%)	16 (84.2%)	5 (41.7%)	0.021
ECOG performance status score, N (%)				
0	22 (71.0%)	16 (84.2%)	6 (50.0%)	
1 or 2	9 (29.0%)	3 (15.8%)	6 (50.0%)	0.056
Baseline PSA (ng/mL)				
median (range)	44.3 (4.3–3204.2)	29.8 (4.3–452.0)	144.3 (14.5–3204.2)	0.047
Baseline alkaline phosphatase (U/L)				
median (range)	108 (58–872)	91 (58–872)	110 (82–744)	0.282
Baseline AR-FL level (copy number)				
median (range)	10 (0–734)	4 (0–121)	26 (3–734)	0.003

* P-value is based on Fisher's Exact test and Wilcoxon Mann-Whitney test for categorical and continuous variables, respectively.

Table S1 B. Baseline characteristics of the 31 patients treated with abiraterone.

Baseline Characteristic	All Patients (N=31)	AR-V7 Negative (N=25)	AR-V7 Positive (N=6)	P-value*
Age (years)				
median (range)	69 (48–79)	69 (48–79)	69 (58–79)	0.565
Race, N (%)				
white	25 (80.6%)	20 (80.0%)	5 (83.3%)	
non-white	6 (19.4%)	5 (20.0%)	1 (16.7%)	0.999
Time since diagnosis (years)				
median (range)	5 (1–21)	5 (1–13)	4 (1–21)	0.705
Tumor stage at diagnosis, N (%)				
T1/T2	12 (38.7%)	10 (40.0%)	2 (33.3%)	
T3/T4	19 (61.3%)	15 (60.0%)	4 (66.7%)	0.999
Gleason sum at diagnosis, N (%)				
≤7	8 (26.7%)	6 (24.0%)	2 (40.0%)	
≥8	22 (73.3%)	19 (76.0%)	3 (60.0%)	0.589
Type of local treatment, N (%)				
surgery	14 (45.2%)	10 (40.0%)	4 (66.6%)	
radiation	10 (32.3%)	9 (36.0%)	1 (16.7%)	
none	7 (22.6%)	6 (24.0%)	1 (16.7%)	0.520
Number of prior hormonal therapies				
mean (range)	2.5 (2–6)	2.2 (2–4)	3.7 (2–6)	0.020
Prior use of enzalutamide, N (%)				
yes	4 (12.9%)	2 (8.0%)	2 (33.3%)	
no	27 (87.1%)	23 (92.0%)	4 (66.7%)	0.159
Prior use of docetaxel, N (%)				
yes	5 (16.1%)	4 (16.0%)	1 (16.7%)	
no	26 (83.9%)	21 (84.0%)	5 (83.3%)	0.999
Presence of bone metastases, N (%)				
yes	24 (77.4%)	19 (76.0%)	5 (83.3%)	
no	7 (22.6%)	6 (24.0%)	1 (16.7%)	0.999
Number of bone metastases, N (%)				
≤5	17 (54.8%)	15 (60.0%)	2 (33.3%)	
≥6	14 (45.2%)	10 (40.4%)	4 (66.7%)	0.370
Presence of visceral metastases, N (%)				
yes	8 (25.8%)	8 (32.0%)	0 (0%)	
no	23 (74.2%)	17 (68.0%)	6 (100%)	0.298
ECOG performance status score, N (%)				
0	25 (80.6%)	22 (88.0%)	3 (50.0%)	
1 or 2	6 (19.4%)	3 (12.0%)	3 (50.0%)	0.069
Baseline PSA (ng/mL)				
median (range)	37.8 (2.2–2045.0)	31.4 (2.2–262.2)	86.9 (19.4–2045.0)	0.084
Baseline alkaline phosphatase (U/L)				
median (range)	118 (59-1348)	109 (59–524)	263 (71–1348)	0.063
Baseline AR-FL level (copy number)				
median (range)	3 (0–609)	1 (0–173)	216 (8–609)	0.002

* P-value is based on Fisher's Exact test and Wilcoxon Mann-Whitney test for categorical and continuous variables, respectively.

Table S2. Clinical outcomes (PSA responses, PSA-PFS and PFS) reported separately according to prior exposure to abiraterone (in the enzalutamide cohort) and prior exposure to enzalutamide (in the abiraterone cohort).

A. Enzalutamide cohort: Clinical outcomes according to prior exposure (or not) to abiraterone

Outcome	**No previous abiraterone** (n=11)			**Previous abiraterone** (n=20)		
	AR-V7 [+] (n=1)	AR-V7 [–] (n=10)	*P* value	AR-V7 [+] (n=11)	AR-V7 [–] (n=9)	*P* value
PSA Response	0% (0/1)	80% (8/10)	0.273	0% (0/11)	22% (2/9)	0.189
PFA-PFS	HR (95%CI) not estimable		0.005	HR 3.34 (95%CI, 1.14–9.80)		0.021
PFS	HR (95%CI) not estimable		0.005	HR 2.93 (95%CI, 0.96–8.90)		0.048

B. Abiraterone cohort: Clinical outcomes according to prior exposure (or not) to enzalutamide

Outcome	**No previous enzalutamide** (n=27)			**Previous enzalutamide** (n=4)		
	AR-V7 [+] (n=4)	AR-V7 [–] (n=23)	*P* value	AR-V7 [+] (n=2)	AR-V7 [–] (n=2)	*P* value
PSA Response	0% (0/4)	74% (17/23)	0.012	0% (0/2)	0% (0/2)	N/A
PFA-PFS	HR 41.0 (95%CI, 4.5–376.8)		<0.001	HR (95%CI) not estimable		N/A
PFS	HR 28.2 (95%CI, 3.1–255.8)		<0.001	HR (95%CI) not estimable		N/A

C. Combined cohort: Clinical outcomes according to prior exposure to abiraterone/enzalutamide

Outcome	**No prior abiraterone/enzalutamide** (n=38)			**Prior abiraterone/enzalutamide** (n=24)		
	AR-V7 [+] (n=5)	AR-V7 [–] (n=33)	*P* value	AR-V7 [+] (n=13)	AR-V7 [–] (n=11)	*P* value
PSA Response	0% (0/5)	76% (25/33)	0.003	0% (0/13)	18% (2/11)	0.199
PFA-PFS	HR 55.9 (95%CI, 6.4–488.5)		<0.001	HR 2.91 (95%CI, 1.10–7.72)		0.023
PFS	HR 45.2 (95%CI, 5.1–398.1)		<0.001	HR 2.65 (95%CI, 0.97–7.25)		0.048

Table S3. Propensity score weighted multivariable Cox models adjusted for Gleason score, baseline PSA, number of prior hormonal treatments, presence of visceral metastases, ECOG score, prior abiraterone/enzalutamide use, and AR-FL levels.

A. Propensity score weighted multivariable Cox model for PSA-PFS in enzalutamide-treated men

Variable	Hazard Ratio (HR)	95% Confidence Interval (95% CI)	*P* value
AR-V7 Positive	3.40	(1.43 – 8.08)	0.006
AR-FL Level (log)	1.33	(1.03 – 1.72)	
Prior use of Abiraterone	2.66	(0.72 – 9.86)	

B. Propensity score weighted multivariable Cox model for PFS in enzalutamide-treated men

Variable	Hazard Ratio (HR)	95% Confidence Interval (95% CI)	*P* value
AR-V7 Positive	3.38	(1.35 – 8.46)	0.009
AR-FL Level (log)	1.64	(1.14 – 2.35)	
Prior use of Abiraterone	1.54	(0.31 – 7.79)	

C. Propensity score weighted multivariable Cox model for PSA-PFS in abiraterone-treated men

Variable	Hazard Ratio (HR)	95% Confidence Interval (95% CI)	*P* value
AR-V7 Positive	17.51	(3.53 – 87.03)	<0.001
AR-FL Level (log)	1.05	(0.87 – 1.25)	
Prior use of Enzalutamide	0.61	(0.17 – 2.19)	

D. Propensity score weighted multivariable Cox model for PFS in abiraterone-treated men

Variable	Hazard Ratio (HR)	95% Confidence Interval (95% CI)	*P* value
AR-V7 Positive	5.25	(1.09 – 25.21)	0.038
AR-FL Level (log)	1.36	(0.97 – 1.90)	
Prior use of Enzalutamide	1.72	(0.50 – 5.92)	

Table S4. Clinical outcomes (PSA responses, PSA-PFS and PFS) for the entire patient population according to their AR-V7 'conversion' rates.

Footnote: Of the 44 patients who were AR-V7–negative at baseline, 42 had at least one follow-up sample collected; 36 of these men (86%) remained AR-V7–negative at follow-up (AR-V7[–] → AR-V7[–]), while 6 of these men (14%) converted to AR-V7–positive at follow-up (AR-V7[–] → AR-V7[+]). Of the 18 patients who were AR-V7–positive at baseline, 16 had at least one follow-up sample collected; all of these men remained AR-V7–positive at follow-up (AR-V7[+] → AR-V7[+]). The clinical outcomes of these patients are also shown.

These data should be interpreted with caution (and are hypothesis-generating only) because we have not taken into account the timing of the subsequent sample collection, and we have not performed time-dependent covariate analysis or landmark analysis to adjust for this. Therefore, the clinical outcomes in each group cannot be formally compared with each other, and are provided for descriptive purposes only.

Outcome	**AR-V7[–] → AR-V7[–]** (n=36)	**AR-V7[–] → AR-V7[+]** (n=6)	**AR-V7[+] → AR-V7[+]** (n=16)
PSA Response	68% (95%CI, 52 – 81%)	17% (95%CI, 4 – 58%)	0% (95%CI, 0 – 19%)
PFA-PFS	6.1 months (95%CI, 5.9 mo – NA)	3.0 months (95%CI, 2.3 mo – NA)	1.4 months (95%CI, 0.9 – 2.6 mo)
PFS	6.5 months (95%CI, 6.1 mo – NA)	3.2 months (95%CI, 3.1 mo – NA)	2.1 months (95%CI, 1.9 – 3.1 mo)

Table S5. Expression profiles of AR-regulated genes in AR-V7–positive and AR-V7–negative metastatic tumors.

Footnote: A total of 34 canonical AR regulated genes were identified by combined analysis of downloaded expression data reported in two published studies.[1,11] The AR gene did not make the selection but was added for reference. For each of the 35 genes, the number of raw RNA-Seq reads and sequencing reads normalized by "Reads Per Kilo Gene Size Per Million of Total Reads" (RPKM= number of raw counts/(gene-length/1000)/(total-reads/1,000,000) in each of the four tumor samples, as well as the log fold expression change between AR-V7-positive and AR-V7-negative tumors calculated from RPKM-normalized data, are displayed. Annexed to the RNA-Seq data are previously published expression microarray data [4] characterizing AR-V7– versus AR-FL–driven transcriptional programs (expression ratios normalized to a common reference sample were downloaded from GEO accession number GSE36549). Fold expression changes in AR-V7–positive samples when compared to AR-V7–negative tumors (log FC) are significantly correlated ($P<0.001$, with a correlation coefficient of 0.68) with fold expression changes induced by AR-V7 in the absence of AR-FL activation (log FC by ARV7), but not significantly correlated ($p>0.05$, with a correlation coefficient of 0.23) with fold expression changes induced by AR-FL activation (log FC by ARFL).

Gene	Size (bp)	Raw V7(–) Met 1	Raw V7(–) Met 2	Raw V7(+) Met 1	Raw V7(+) Met 2	RPKM V7(–) Met 1	RPKM V7(–) Met 2	RPKM V7(+) Met 1	RPKM V7(+) Met 2	log FC	CSS	R1881	CSS + ARV7	R1881 + ARV7	log FC by ARV7	log FC by ARFL
AR	4496	23044	20645	21722	62370	111.83	92.43	54.53	201.92	-0.22	0.10	-0.89	-0.01	-0.96	-0.11	-0.99
C1orf116	5502	3123	5063	3293	10168	12.38	18.52	6.75	26.90	-0.62	-0.90	1.05	-0.90	0.99	0.01	1.95
CENPN	5307	1337	11671	1799	907	5.50	44.27	3.83	2.49	-3.26	-2.67	0.52	-1.92	0.88	0.75	3.20
CXCR4	2005	654	695	10593	7739	7.12	6.98	59.63	56.18	2.65	-0.40	2.77	-0.26	3.51	0.13	3.17
DBI	1260	11624	10108	43384	10800	201.28	161.47	388.60	124.76	0.11	-0.50	3.07	0.33	3.19	0.82	3.57
EAF2	1020	66	212	3689	116	1.41	4.18	40.82	1.66	0.74	0.10	4.18	0.37	3.77	0.28	4.08
EBP	1157	784	3333	3322	2755	14.78	57.98	32.40	34.66	-0.20	-0.48	0.88	-0.07	0.75	0.41	1.35
FASN	8458	2272	5891	19983	46976	5.86	14.02	26.66	80.84	1.97	-0.50	0.61	-0.06	0.86	0.44	1.11
FKBP5	10628	3810	34978	55568	66987	7.82	66.24	59.01	91.74	1.32	-1.28	3.61	1.26	4.03	2.54	4.89
FZD5	6564	3247	6014	3756	2384	10.79	18.44	6.46	5.29	-1.98	-1.12	1.65	-0.93	1.80	0.19	2.77

HMGCR	4582	2395	3169	3526	2334	11.40	13.92	8.68	7.41	-1.25	0.06	1.54	0.07	1.27	0.01	1.49
HMGCS1	3510	2596	5207	12367	3282	16.14	29.86	39.76	13.61	-0.38	0.40	2.15	0.65	1.79	0.25	1.75
HPGD	3022	127	57	392	29067	0.92	0.38	1.46	140.00	3.64	-2.52	3.46	-0.05	4.05	2.47	5.98
INSIG1	3081	421	3684	3118	8029	2.98	24.07	11.42	37.93	0.90	-0.58	1.55	0.27	2.00	0.85	2.13
KLK2	2872	286904	327838	82985	16542	2179.51	2297.62	326.10	83.84	-3.76	-4.34	0.14	-3.86	0.37	0.48	4.48
KLK3	2214	213712	922556	121923	32693	2106.00	8387.23	621.51	214.93	-3.03	-3.75	-0.16	-2.95	0.37	0.80	3.59
KLK4	1347	2478	3956	813	4579	40.14	59.11	6.81	49.48	-1.81	-2.68	-0.19	-2.59	-0.20	0.08	2.49
LDLR	5283	149	1947	2714	5261	0.62	7.42	5.80	14.49	1.47	-0.82	1.70	-0.23	1.50	0.60	2.52
MAF	6878	425	778	4311	1659	1.35	2.28	7.07	3.51	0.59	-1.22	2.98	-1.54	2.81	-0.32	4.20
MICAL1	3644	685	88	2959	2630	4.10	0.49	9.16	10.51	2.00	0.32	3.28	0.28	3.14	-0.04	2.96
NCAPD3	5605	849	1024	2601	4880	3.30	3.68	5.24	12.67	0.63	-0.62	2.50	-0.22	2.55	0.41	3.12
NDRG1	3478	66845	19467	44162	124199	419.32	112.66	143.30	519.78	0.22	-1.02	2.99	0.11	3.35	1.14	4.01
NKX3-1	3281	35635	53042	44160	43298	236.96	325.40	151.90	192.08	-0.89	-2.62	1.17	-2.59	1.04	0.04	3.80
ORM1	839	3	2407	94992	21539	0.08	57.75	1277.81	373.67	7.90	-0.88	4.10	6.70	6.47	7.57	4.97
PMEPA1	5186	10061	16129	7660	5565	42.33	62.60	16.67	15.62	-2.12	-1.49	1.04	-0.81	1.22	0.67	2.52
PTPN21	6215	551	1684	565	2532	1.93	5.45	1.03	5.93	-1.28	1.08	3.51	0.84	3.47	-0.24	2.43
RAB3B	12844	2274	10492	8012	3620	3.86	16.44	7.04	4.10	-1.33	-1.39	1.25	-1.14	1.22	0.25	2.64
RHOU	4758	16379	28644	5876	7735	75.11	121.17	13.94	23.66	-2.77	0.28	3.58	0.34	3.71	0.06	3.30
SCAP	4255	609	869	1134	4593	3.12	4.11	3.01	15.71	0.34	-0.29	0.76	-0.11	0.99	0.18	1.05
SGK1	3965	105	24777	20302	1347	0.58	125.78	57.79	4.94	0.24	-0.10	3.35	-0.05	3.62	0.05	3.45
SLC45A3	3382	5108	7039	2578	15489	32.95	41.89	8.60	66.66	-1.03	-2.52	1.07	-2.29	1.42	0.23	3.59
TMPRSS2	3320	4457	54020	27831	19920	29.29	327.51	94.61	87.33	-0.53	-4.59	-0.38	-3.92	0.09	0.67	4.21
WIPI1	1924	209	435	6828	1472	2.37	4.55	40.05	11.14	2.15	-0.10	2.57	0.98	2.86	1.08	2.67
WWC1	6739	2465	1922	6536	5735	7.98	5.74	10.95	12.39	0.26	-0.75	0.16	-0.99	0.21	-0.23	0.91
ZNF350	2341	2985	3161	5862	1155	27.82	27.18	28.26	7.18	-1.54	0.27	1.27	0.18	1.35	-0.09	1.00

Table S6. R^2 values for regression models that include only AR-FL levels (continuous variable) compared to regression models that additionally include AR-V7 status, for each clinical outcome (PSA response rate, PSA-PFS and PFS).

Footnote: The R^2 values are based on the Sums-of-squares method of Mittleböck and Schemper (Computing measures of explained variation for logistic regression models. Computer Methods and Programs in Biomedicine 1999; 58:17-24) for PSA response rate, and on the method of Heller (A measure of explained risk in the proportional hazards model. Biostatistics 2012; 13:315-325) for PSA-PFS and PFS. P-values are based on the Likelihood ratio test.

Outcome	**Regression Models – Enzalutamide Cohort**			**Regression Models – Abiraterone Cohort**		
	AR-FL alone	AR-FL + AR-V7	*P* value	AR-FL alone	AR-FL + AR-V7	*P* value
PSA Response	$R^2 = 0.307$	$R^2 = 0.449$	0.019	$R^2 = 0.203$	$R^2 = 0.336$	0.021
PFA-PFS	$R^2 = 0.196$	$R^2 = 0.573$	<0.001	$R^2 = 0.651$	$R^2 = 0.793$	0.012
PFS	$R^2 = 0.341$	$R^2 = 0.649$	<0.001	$R^2 = 0.869$	$R^2 = 0.903$	0.083

Supplementary References

1. Hu R, Dunn TA, Wei S, et al. Ligand-independent androgen receptor variants derived from splicing of cryptic exons signify hormone-refractory prostate cancer. Cancer Res 2009;69:16-22.
2. Watson PA, Chen YF, Balbas MD, et al. Constitutively active androgen receptor splice variants expressed in castration-resistant prostate cancer require full-length androgen receptor. Proceedings of the National Academy of Sciences 2010.
3. Hu R, Isaacs WB, Luo J. A snapshot of the expression signature of androgen receptor splicing variants and their distinctive transcriptional activities. The Prostate 2011;71:1656-67.
4. Hu R, Lu C, Mostaghel EA, et al. Distinct transcriptional programs mediated by the ligand-dependent full-length androgen receptor and its splice variants in castration-resistant prostate cancer. Cancer Res 2012;72:3457-62.
5. Luo J, Duggan DJ, Chen Y, et al. Human prostate cancer and benign prostatic hyperplasia: molecular dissection by gene expression profiling. Cancer Res 2001;61:4683-8.
6. Aryee MJ, Liu W, Engelmann JC, et al. DNA methylation alterations exhibit intraindividual stability and interindividual heterogeneity in prostate cancer metastases. Science translational medicine 2013;5:169ra10.
7. Liu W, Laitinen S, Khan S, et al. Copy number analysis indicates monoclonal origin of lethal metastatic prostate cancer. Nature medicine 2009;15:559-65.
8. Robinson JT, Thorvaldsdottir H, Winckler W, et al. Integrative genomics viewer. Nature biotechnology 2011;29:24-6.
9. Anders S, Pyl PT, Huber W. HTSeq–A Python framework to work with high-throughput sequencing data. bioRxiv 2014.
10. Subramanian A, Tamayo P, Mootha VK, et al. Gene set enrichment analysis: a knowledge-based approach for interpreting genome-wide expression profiles. Proceedings of the National Academy of Sciences of the United States of America 2005;102:15545-50.
11. Norris JD, Chang CY, Wittmann BM, et al. The homeodomain protein HOXB13 regulates the cellular response to androgens. Molecular cell 2009;36:405-16.